Observation of η^{′}→ωe^{+}e^{-}

M. Ablikim *et al.* (BESIII Collaboration)

Phys. Rev. D **92**, 051101 — Published 14 September 2015

DOI: 10.1103/PhysRevD.92.051101

Observation of $\eta' \to \omega e^+ e^-$

M. Ablikim[1], M. N. Achasov[9,f], X. C. Ai[1], O. Albayrak[5], M. Albrecht[4], D. J. Ambrose[44], A. Amoroso[49A,49C], F. F. An[1], Q. An[46,a], J. Z. Bai[1], R. Baldini Ferroli[20A], Y. Ban[31], D. W. Bennett[19], J. V. Bennett[5], M. Bertani[20A], D. Bettoni[21A], J. M. Bian[43], F. Bianchi[49A,49C], E. Boger[23,d], I. Boyko[23], R. A. Briere[5], H. Cai[51], X. Cai[1,a], O. Cakir[40A,b], A. Calcaterra[20A], G. F. Cao[1], S. A. Cetin[40B], J. F. Chang[1,a], G. Chelkov[23,d,e], G. Chen[1], H. S. Chen[1], H. Y. Chen[2], J. C. Chen[1], M. L. Chen[1,a], S. J. Chen[29], X. Chen[1,a], X. R. Chen[26], Y. B. Chen[1,a], H. P. Cheng[17], X. K. Chu[31], G. Cibinetto[21A], H. L. Dai[1,a], J. P. Dai[34], A. Dbeyssi[14], D. Dedovich[23], Z. Y. Deng[1], A. Denig[22], I. Denysenko[23], M. Destefanis[49A,49C], F. De Mori[49A,49C], Y. Ding[27], C. Dong[30], J. Dong[1,a], L. Y. Dong[1], M. Y. Dong[1,a], S. X. Du[53], P. F. Duan[1], E. E. Eren[40B], J. Z. Fan[39], J. Fang[1,a], S. S. Fang[1], X. Fang[46,a], Y. Fang[1], L. Fava[49B,49C], F. Feldbauer[22], G. Felici[20A], C. Q. Feng[46,a], E. Fioravanti[21A], M. Fritsch[14,22], C. D. Fu[1], Q. Gao[1], X. Y. Gao[2], Y. Gao[39], Z. Gao[46,a], I. Garzia[21A], K. Goetzen[10], W. X. Gong[1,a], W. Gradl[22], M. Greco[49A,49C], M. H. Gu[1,a], Y. T. Gu[12], Y. H. Guan[1], A. Q. Guo[1], L. B. Guo[28], Y. Guo[1], Y. P. Guo[22], Z. Haddadi[25], A. Hafner[22], S. Han[51], X. Q. Hao[15], F. A. Harris[42], K. L. He[1], X. Q. He[45], T. Held[4], Y. K. Heng[1,a], Z. L. Hou[1], C. Hu[28], H. M. Hu[1], J. F. Hu[49A,49C], T. Hu[1,a], Y. Hu[1], G. M. Huang[6], G. S. Huang[46,a], J. S. Huang[15], X. T. Huang[33], Y. Huang[29], T. Hussain[48], Q. Ji[1], Q. P. Ji[30], X. B. Ji[1], X. L. Ji[1,a], L. W. Jiang[51], X. S. Jiang[1,a], X. Y. Jiang[30], J. B. Jiao[33], Z. Jiao[17], D. P. Jin[1,a], S. Jin[1], T. Johansson[50], A. Julin[43], N. Kalantar-Nayestanaki[25], X. L. Kang[1], X. S. Kang[30], M. Kavatsyuk[25], B. C. Ke[5], P. Kiese[22], R. Kliemt[14], B. Kloss[22], O. B. Kolcu[40B,i], B. Kopf[4], M. Kornicer[42], W. Kühn[24], A. Kupsc[50], J. S. Lange[24], M. Lara[19], P. Larin[14], C. Leng[49C], C. Li[50], Cheng Li[46,a], D. M. Li[53], F. Li[1,a], F. Y. Li[31], G. Li[1], H. B. Li[1], J. C. Li[1], Jin Li[32], K. Li[33], K. Li[13], Lei Li[3], P. R. Li[41], T. Li[33], W. D. Li[1], W. G. Li[1], X. L. Li[33], X. M. Li[12], X. N. Li[1,a], X. Q. Li[30], Z. B. Li[38], H. Liang[46,a], Y. F. Liang[36], Y. T. Liang[24], G. R. Liao[11], D. X. Lin[14], B. J. Liu[1], C. X. Liu[1], F. H. Liu[35], Fang Liu[1], Feng Liu[6], H. B. Liu[12], H. H. Liu[16], H. H. Liu[1], H. M. Liu[1], J. Liu[1], J. B. Liu[46,a], J. P. Liu[51], J. Y. Liu[1], K. Liu[39], K. Y. Liu[27], L. D. Liu[31], P. L. Liu[1,a], Q. Liu[41], S. B. Liu[46,a], X. Liu[26], Y. B. Liu[30], Z. A. Liu[1,a], Zhiqing Liu[22], H. Loehner[25], X. C. Lou[1,a,h], H. J. Lu[17], J. G. Lu[1,a], Y. Lu[1], Y. P. Lu[1,a], C. L. Luo[28], M. X. Luo[52], T. Luo[42], X. L. Luo[1,a], X. R. Lyu[41], F. C. Ma[27], H. L. Ma[1], L. L. Ma[33], Q. M. Ma[1], T. Ma[1], X. N. Ma[30], X. Y. Ma[1,a], F. E. Maas[14], M. Maggiora[49A,49C], Y. J. Mao[31], Z. P. Mao[1], S. Marcello[49A,49C], J. G. Messchendorp[25], J. Min[1,a], R. E. Mitchell[19], X. H. Mo[1,a], Y. J. Mo[6], C. Morales Morales[14], K. Moriya[19], N. Yu. Muchnoi[9,f], H. Muramatsu[43], Y. Nefedov[23], F. Nerling[14], I. B. Nikolaev[9,f], Z. Ning[1,a], S. Nisar[8], S. L. Niu[1,a], X. Y. Niu[1], S. L. Olsen[32], Q. Ouyang[1,a], S. Pacetti[20B], P. Patteri[20A], M. Pelizaeus[4], H. P. Peng[46,a], K. Peters[10], J. Pettersson[50], J. L. Ping[28], R. G. Ping[1], R. Poling[43], V. Prasad[1], M. Qi[29], S. Qian[1,a], C. F. Qiao[41], L. Q. Qin[33], N. Qin[51], X. S. Qin[1], Z. H. Qin[1,a], J. F. Qiu[1], K. H. Rashid[48], C. F. Redmer[22], M. Ripka[22], G. Rong[1], Ch. Rosner[14], X. D. Ruan[12], V. Santoro[21A], A. Sarantsev[23,g], M. Savrié[21B], K. Schoenning[50], S. Schumann[22], W. Shan[31], M. Shao[46,a], C. P. Shen[2], P. X. Shen[30], X. Y. Shen[1], H. Y. Sheng[1], W. M. Song[1], X. Y. Song[1], S. Sosio[49A,49C], S. Spataro[49A,49C], G. X. Sun[1], J. F. Sun[15], S. S. Sun[1], Y. J. Sun[46,a], Y. Z. Sun[1], Z. J. Sun[1,a], Z. T. Sun[19], C. J. Tang[36], X. Tang[1], I. Tapan[40C], E. H. Thorndike[44], M. Tiemens[25], M. Ullrich[24], I. Uman[40B], G. S. Varner[42], B. Wang[30], D. Wang[31], D. Y. Wang[31], K. Wang[1,a], L. L. Wang[1], L. S. Wang[1], M. Wang[33], P. Wang[1], P. L. Wang[1], S. G. Wang[31], W. Wang[1,a], X. F. Wang[39], Y. D. Wang[14], Y. F. Wang[1,a], Y. Q. Wang[22], Z. Wang[1,a], Z. G. Wang[1,a], Z. H. Wang[46,a], Z. Y. Wang[1], T. Weber[22], D. H. Wei[11], J. B. Wei[31], P. Weidenkaff[22], S. P. Wen[1], U. Wiedner[4], M. Wolke[50], L. H. Wu[1], Z. Wu[1,a], L. G. Xia[39], Y. Xia[18], D. Xiao[1], H. Xiao[47], Z. J. Xiao[28], Y. G. Xie[1,a], Q. L. Xiu[1,a], G. F. Xu[1], L. Xu[1], Q. J. Xu[13], X. P. Xu[37], L. Yan[46,a], W. B. Yan[46,a], W. C. Yan[46,a], Y. H. Yan[18], H. J. Yang[34], H. X. Yang[1], L. Yang[51], Y. Yang[6], Y. X. Yang[11], M. Ye[1,a], M. H. Ye[7], J. H. Yin[1], B. X. Yu[1,a], C. X. Yu[30], J. S. Yu[26], C. Z. Yuan[1], W. L. Yuan[29], Y. Yuan[1], A. Yuncu[40B,c], A. A. Zafar[48], A. Zallo[20A], Y. Zeng[18], B. X. Zhang[1], B. Y. Zhang[1,a], C. Zhang[29], C. C. Zhang[1], D. H. Zhang[1], H. H. Zhang[38], H. Y. Zhang[1,a], J. J. Zhang[1], J. L. Zhang[1], J. Q. Zhang[1], J. W. Zhang[1,a], J. Y. Zhang[1], J. Z. Zhang[1], K. Zhang[1], L. Zhang[1], X. Y. Zhang[33], Y. Zhang[1], Y. N. Zhang[41], Y. H. Zhang[1,a], Y. T. Zhang[46,a], Yu Zhang[41], Z. H. Zhang[6], Z. P. Zhang[46], Z. Y. Zhang[51], G. Zhao[1], J. W. Zhao[1,a], J. Y. Zhao[1], J. Z. Zhao[1,a], Lei Zhao[46,a], Ling Zhao[1], M. G. Zhao[30], Q. Zhao[1], Q. W. Zhao[1], S. J. Zhao[53], T. C. Zhao[1], Y. B. Zhao[1,a], Z. G. Zhao[46,a], A. Zhemchugov[23,d], B. Zheng[47], J. P. Zheng[1,a], W. J. Zheng[33], Y. H. Zheng[41], B. Zhong[28], L. Zhou[1,a], X. Zhou[51], X. K. Zhou[46,a], X. R. Zhou[46,a], X. Y. Zhou[1], K. Zhu[1], K. J. Zhu[1,a], S. Zhu[1], S. H. Zhu[45], X. L. Zhu[39], Y. C. Zhu[46,a], Y. S. Zhu[1], Z. A. Zhu[1], J. Zhuang[1,a], L. Zotti[49A,49C], B. S. Zou[1], J. H. Zou[1]

(BESIII Collaboration)

[1] *Institute of High Energy Physics, Beijing 100049, People's Republic of China*
[2] *Beihang University, Beijing 100191, People's Republic of China*
[3] *Beijing Institute of Petrochemical Technology, Beijing 102617, People's Republic of China*
[4] *Bochum Ruhr-University, D-44780 Bochum, Germany*
[5] *Carnegie Mellon University, Pittsburgh, Pennsylvania 15213, USA*
[6] *Central China Normal University, Wuhan 430079, People's Republic of China*
[7] *China Center of Advanced Science and Technology, Beijing 100190, People's Republic of China*
[8] *COMSATS Institute of Information Technology, Lahore, Defence Road, Off Raiwind Road, 54000 Lahore, Pakistan*
[9] *G.I. Budker Institute of Nuclear Physics SB RAS (BINP), Novosibirsk 630090, Russia*
[10] *GSI Helmholtzcentre for Heavy Ion Research GmbH, D-64291 Darmstadt, Germany*
[11] *Guangxi Normal University, Guilin 541004, People's Republic of China*
[12] *GuangXi University, Nanning 530004, People's Republic of China*
[13] *Hangzhou Normal University, Hangzhou 310036, People's Republic of China*

[14] Helmholtz Institute Mainz, Johann-Joachim-Becher-Weg 45, D-55099 Mainz, Germany
[15] Henan Normal University, Xinxiang 453007, People's Republic of China
[16] Henan University of Science and Technology, Luoyang 471003, People's Republic of China
[17] Huangshan College, Huangshan 245000, People's Republic of China
[18] Hunan University, Changsha 410082, People's Republic of China
[19] Indiana University, Bloomington, Indiana 47405, USA
[20] (A)INFN Laboratori Nazionali di Frascati, I-00044, Frascati, Italy; (B)INFN and University of Perugia, I-06100, Perugia, Italy
[21] (A)INFN Sezione di Ferrara, I-44122, Ferrara, Italy; (B)University of Ferrara, I-44122, Ferrara, Italy
[22] Johannes Gutenberg University of Mainz, Johann-Joachim-Becher-Weg 45, D-55099 Mainz, Germany
[23] Joint Institute for Nuclear Research, 141980 Dubna, Moscow region, Russia
[24] Justus Liebig University Giessen, II. Physikalisches Institut, Heinrich-Buff-Ring 16, D-35392 Giessen, Germany
[25] KVI-CART, University of Groningen, NL-9747 AA Groningen, The Netherlands
[26] Lanzhou University, Lanzhou 730000, People's Republic of China
[27] Liaoning University, Shenyang 110036, People's Republic of China
[28] Nanjing Normal University, Nanjing 210023, People's Republic of China
[29] Nanjing University, Nanjing 210093, People's Republic of China
[30] Nankai University, Tianjin 300071, People's Republic of China
[31] Peking University, Beijing 100871, People's Republic of China
[32] Seoul National University, Seoul, 151-747 Korea
[33] Shandong University, Jinan 250100, People's Republic of China
[34] Shanghai Jiao Tong University, Shanghai 200240, People's Republic of China
[35] Shanxi University, Taiyuan 030006, People's Republic of China
[36] Sichuan University, Chengdu 610064, People's Republic of China
[37] Soochow University, Suzhou 215006, People's Republic of China
[38] Sun Yat-Sen University, Guangzhou 510275, People's Republic of China
[39] Tsinghua University, Beijing 100084, People's Republic of China
[40] (A)Istanbul Aydin University, 34295 Sefakoy, Istanbul, Turkey; (B)Dogus University, 34722 Istanbul, Turkey; (C)Uludag University, 16059 Bursa, Turkey
[41] University of Chinese Academy of Sciences, Beijing 100049, People's Republic of China
[42] University of Hawaii, Honolulu, Hawaii 96822, USA
[43] University of Minnesota, Minneapolis, Minnesota 55455, USA
[44] University of Rochester, Rochester, New York 14627, USA
[45] University of Science and Technology Liaoning, Anshan 114051, People's Republic of China
[46] University of Science and Technology of China, Hefei 230026, People's Republic of China
[47] University of South China, Hengyang 421001, People's Republic of China
[48] University of the Punjab, Lahore-54590, Pakistan
[49] (A)University of Turin, I-10125, Turin, Italy; (B)University of Eastern Piedmont, I-15121, Alessandria, Italy; (C)INFN, I-10125, Turin, Italy
[50] Uppsala University, Box 516, SE-75120 Uppsala, Sweden
[51] Wuhan University, Wuhan 430072, People's Republic of China
[52] Zhejiang University, Hangzhou 310027, People's Republic of China
[53] Zhengzhou University, Zhengzhou 450001, People's Republic of China

[a] Also at State Key Laboratory of Particle Detection and Electronics, Beijing 100049, Hefei 230026, People's Republic of China
[b] Also at Ankara University,06100 Tandogan, Ankara, Turkey
[c] Also at Bogazici University, 34342 Istanbul, Turkey
[d] Also at the Moscow Institute of Physics and Technology, Moscow 141700, Russia
[e] Also at the Functional Electronics Laboratory, Tomsk State University, Tomsk, 634050, Russia
[f] Also at the Novosibirsk State University, Novosibirsk, 630090, Russia
[g] Also at the NRC "Kurchatov Institute, PNPI, 188300, Gatchina, Russia
[h] Also at University of Texas at Dallas, Richardson, Texas 75083, USA
[i] Also at Istanbul Arel University, 34295 Istanbul, Turkey

Based on a sample of η' mesons produced in the radiative decay $J/\psi \to \gamma\eta'$ in 1.31×10^9 J/ψ events collected with the BESIII detector, the decay $\eta' \to \omega e^+e^-$ is observed for the first time, with a statistical significance of 8σ. The branching fraction is measured to be $\mathcal{B}(\eta' \to \omega e^+e^-) = (1.97 \pm 0.34(\text{stat}) \pm 0.17(\text{syst})) \times 10^{-4}$, which is in agreement with theoretical predictions. The branching fraction of $\eta' \to \omega\gamma$ is also measured to be $(2.55 \pm 0.03(\text{stat}) \pm 0.16(\text{syst})) \times 10^{-2}$, which is the most precise measurement to date, and the relative branching fraction $\frac{\mathcal{B}(\eta' \to \omega e^+e^-)}{\mathcal{B}(\eta' \to \omega\gamma)}$ is determined to be $(7.71 \pm 1.34(\text{stat}) \pm 0.54(\text{syst})) \times 10^{-3}$.

PACS numbers: 12.40.Vv, 14.40.Be, 13.20.Jf

I. INTRODUCTION

The main decays of the η' meson [1] fall into two distinct classes. The first class consists of hadronic decays into three pseudoscalar mesons, such as $\eta' \to \eta\pi\pi$, while the second class has radiative decays into vector particles with quantum number $J^{PC} = 1^{--}$, such as $\eta' \to \gamma\gamma, \rho\gamma$, or $\omega\gamma$. Model-dependent approaches for describing low energy mesonic interactions, such as vector meson dominance (VMD) [2], and the applicability of chiral perturbation theory [2] can be tested in η' decays.

It is of interest to study the decay $\eta' \to Ve^+e^-$ (V represents vector meson) which proceeds via a two-body radiative decay into a vector meson and an off-shell photon. The electron-positron invariant mass distribution provides information about the intrinsic structure of the η' meson and the momentum dependence of the transition form factor. Recently, BESIII reported the measurement of $\eta' \to \pi^+\pi^-e^+e^-$ [3], which is found to be dominated by $\eta' \to \rho e^+e^-$, in agreement with theoretical predictions [2, 4].

Based on theoretical models [2, 5], the branching fraction of $\eta' \to \omega e^+e^-$ is predicted to be around 2.0×10^{-4}, but until now there has been no measurement of this decay. A sample of 1.31×10^9 J/ψ events (2.25×10^8 events [6] in 2009 and 1.09×10^9 [7] in 2012) has been collected with the BESIII detector and offers us a unique opportunity to investigate η' decays via $J/\psi \to \gamma\eta'$. In this paper, the observation of $\eta' \to \omega e^+e^-$, the analysis of the decay $\eta' \to \omega\gamma$, and the ratio of their branching fractions are reported.

II. DETECTOR AND MONTE CARLO SIMULATION

The BESIII detector is a magnetic spectrometer located at the Beijing Electron Positron Collider (BEPCII, [8]), which is a double-ring e^+e^- collider with a design peak luminosity of 10^{33} cm^{-2} s^{-1} at a center-of-mass energy of 3.773 GeV. The cylindrical core of the BESIII detector consists of a helium-based multilayer drift chamber (MDC), a plastic scintillator time-of-flight system (TOF), and a CsI (Tl) electromagnetic calorimeter (EMC), which are all enclosed in a superconducting solenoidal magnet providing a 1.0 T (0.9 T for the 2012 run period) magnetic field. The solenoid is supported by an octagonal flux-return yoke with modules of resistive plate muon counters (MUC) interleaved with steel. The acceptance for charged particles and photons is 93% of the full 4π solid angle. The momentum resolution for charged particles at 1 GeV/c is 0.5%, and the resolution of the ionization energy loss per unit path-length (dE/dx) is 6%. The EMC measures photon energies with a resolution of 2.5% (5%) at 1 GeV in the barrel (end-caps). The time resolution for the TOF is 80 ps in the barrel and 110 ps in the end-caps. Information from the TOF and dE/dx is combined to perform particle identification (PID).

The estimation of backgrounds and the determinations of detection efficiencies are performed through Monte Carlo (MC) simulations. The BESIII detector is modeled with GEANT4 [9, 10]. The production of the J/ψ resonance is implemented with the MC event generator KKMC [11, 12], while the decays are simulated with EVTGEN [13]. Possible backgrounds are studied using a sample of 'inclusive' J/ψ events of approximately the equivalent luminosity of data, in which the known decays of the J/ψ are modeled with branching fractions being set to the world average values from the Particle Data Group (PDG) [1], while the remaining decays are generated with the LUNDCHARM model [14]. For this analysis, a signal MC sample (6.0×10^5 events), based on the VMD model and chiral perturbation theory [2] for $J/\psi \to \gamma\eta'$, $\eta' \to \omega e^+e^-$, $\omega \to \pi^0\pi^+\pi^-$, $\pi^0 \to \gamma\gamma$, is generated to optimize the selection criteria and determine the detection efficiency.

III. ANALYSIS OF $J/\psi \to \gamma\eta'$

In this analysis, the η' meson is produced in the radiative decay $J/\psi \to \gamma\eta'$. The ω meson is observed in its dominant $\pi^+\pi^-\pi^0$ decay mode, and the π^0 is detected in $\pi^0 \to \gamma\gamma$. Therefore, signal events are observed in the topology $\gamma\gamma\gamma\pi^+\pi^-$ for the $\eta' \to \omega\gamma$ mode, and $\gamma\gamma\gamma\pi^+\pi^-e^+e^-$ for $\eta' \to \omega e^+e^-$. We apply the following basic reconstruction and selection criteria to both channels:

We select tracks in the MDC within the polar angle range $|\cos\theta| < 0.93$ and require that the points of closest approach to the beam line be within ±20 cm of the interaction point in the beam direction and within 2 cm in the plane perpendicular to the beam.

Photon candidates are reconstructed by clustering signals in EMC crystals. At least four photon candidates are required, and the minimum energy of each must be at least 25 MeV for barrel showers ($|\cos\theta| < 0.80$) and 50 MeV for endcap showers ($0.86 < |\cos\theta| < 0.92$). To exclude showers due to the bremsstrahlung of charged particles, the angle between the nearest charged track and the shower must be greater than 10°. To suppress electronics noise and energy deposits unrelated to the event, the EMC cluster time is restricted to be within a 700 ns window near the event start time.

A. $\eta' \to \omega\gamma$

For the decay $\eta' \to \omega\gamma$, two particles with opposite charge are required. No particle identification (PID) is used, and the two tracks are taken to be positive and negative pions from the ω.

A four-constraint (4C) kinematic fit imposing energy-momentum conservation is performed under the hypothesis of $J/\psi \to \gamma\gamma\gamma\gamma\pi^+\pi^-$. If there are more than four photons, the combination with the smallest $\chi^2_{\gamma\gamma\gamma\gamma\pi^+\pi^-}$ is retained. Events with $\chi^2_{\gamma\gamma\gamma\gamma\pi^+\pi^-} < 80$ are retained for further analysis. Since $J/\psi \to \gamma\eta'$ is a two-body decay, the radiative photon carries a unique energy of 1.4 GeV. Hence the photon with maximum energy is taken as the radiative photon, and its energy is required to be greater than 1.0 GeV. The photon pair combination with $\gamma\gamma$ invariant mass closest to the π^0 mass is considered as the π^0 candidate in the final state, and its invariant mass must satisfy $|M(\gamma\gamma) - M_{\pi^0}| < 0.015$ GeV/c^2, where M_{π^0} is the world average value of the π^0 mass [1]. With these requirements, the decay $\eta' \to \omega\gamma$ is observed in the distribution of $M(\pi^0\pi^+\pi^-\gamma)$ versus $M(\pi^0\pi^+\pi^-)$, shown in Fig. 1. Besides the region of interest in Fig. 1 , there is a vertical band around the ω mass region, which comes from $J/\psi \to \omega\eta$, $\omega\pi^0$ and $\omega\pi^0\pi^0$ background, while a horizontal band also exists around the η' mass region, which comes from $J/\psi \to \gamma\eta'$, $\eta' \to \eta\pi^+\pi^-$ and $\gamma\rho^0$.

To improve the mass resolution, as well as to better handle the background in the vertical band around the ω mass region and horizontal band around the η' mass region, we determine the signal yield from the distribution of the difference between $M(\pi^0\pi^+\pi^-\gamma)$ and $M(\pi^0\pi^+\pi^-)$. The backgrounds in the vertical and horizontal bands do not peak in the signal region, which is demonstrated by the inclusive MC sample, as shown by the histogram in Fig. 2.

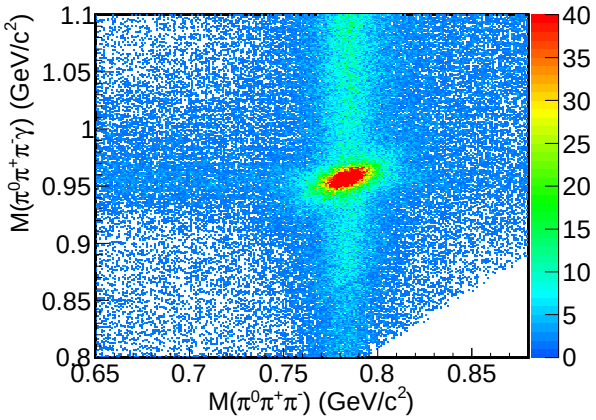

FIG. 1. Distribution of $M(\pi^0\pi^+\pi^-\gamma)$ versus $M(\pi^0\pi^+\pi^-)$ from data.

To determine the signal yield, an unbinned maximum likelihood fit to the mass difference $M(\pi^0\pi^+\pi^-\gamma) - M(\pi^0\pi^+\pi^-)$ is performed, in which the signal shape is described by the MC shape convoluted with a Gaussian function to account for the difference in resolution between data and MC simulation, and the background is described by a 3rd-order Chebychev polynomial. 33187 ± 351 $\eta' \to \omega\gamma$ signal events are obtained from the fit, whose curve is shown in Fig. 2. With the detection efficiency, $(21.87 \pm 0.02)\%$, obtained from MC simulation, the branching fraction, $(2.55 \pm 0.03) \times 10^{-2}$, listed in Table I, is determined.

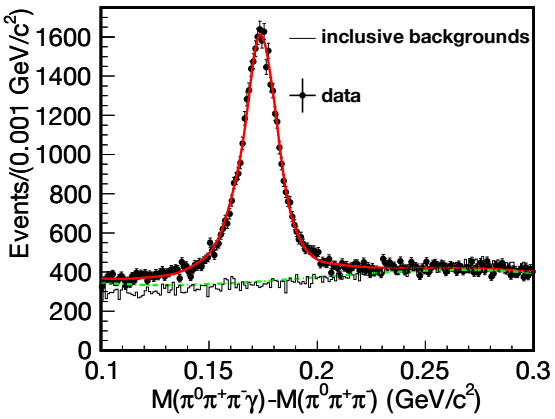

FIG. 2. Distribution of the mass difference $M(\pi^0\pi^+\pi^-\gamma) - M(\pi^0\pi^+\pi^-)$. The dots with error bars are data, the histogram shows the MC simulation of inclusive J/ψ decays. The solid curve represents the fit results, and the dashed curve is the background determined by the fit.

B. $\eta' \to \omega e^+e^-$

For $\eta' \to \omega e^+e^-$ decay, candidate events with four well-reconstructed charged tracks and at least three photons are selected. The charged track and good photon selections are exactly the same as described above.

To select candidate events and select the best photon combination when additional photons are found in an event, the combination with the smallest $\chi^2_{4C+\rm PID}$ is retained. Here $\chi^2_{4C+\rm PID} = \chi^2_{\rm 4C} + \sum_{j=1}^{4} \chi^2_{\rm PID}(j)$ is the sum of the chi-squares from the 4C kinematic fit and from PID, formed by combining TOF and dE/dx information of each charged track for each particle hypothesis (pion, electron, or muon). If the combination with the smallest $\chi^2_{4C+\rm PID}$ corresponds to two oppositely charged pions and an electron and positron, and has $\chi^2_{\rm 4C} < 80$, the event is kept as a $\gamma\gamma\gamma\pi^+\pi^-e^+e^-$ candidate. As in the analysis of $\eta' \to \omega\gamma$, the selected photon with maximum energy is taken as the radiative photon, and its energy is required to be greater than 1.0 GeV. The other two photons are further required to be consistent with a π^0 candidate, $|M(\gamma\gamma) - M_{\pi^0}| < 0.015$ GeV/c^2.

With the above selection criteria, MC simulation shows

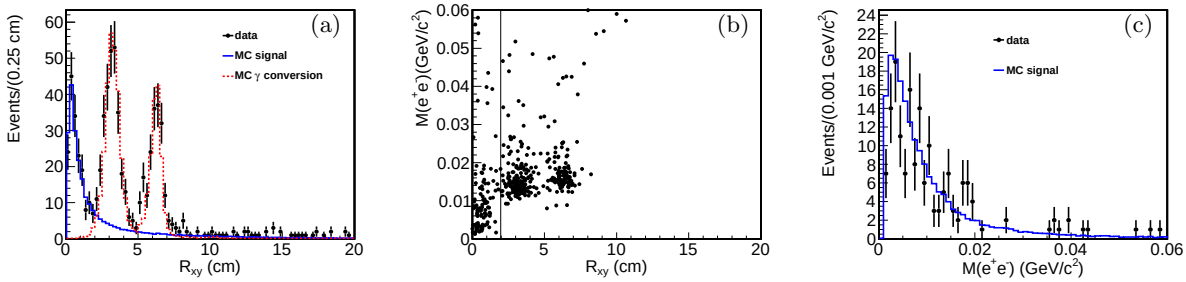

FIG. 3. (a) Distribution of the distance of the reconstructed e^+e^- vertex from the z axis, R_{xy}, where the dots with error bars are data, the solid histogram is signal MC simulation, and the dotted histogram is MC simulation of $\eta' \to \omega\gamma$. (b) Distribution of $M(e^+e^-)$ versus R_{xy}, where the requirement of $R_{xy} < 2$ cm is indicated as the vertical line. (c) Distribution of $M(e^+e^-)$ with the requirement $R_{xy} < 2$ cm, where the dots with error bars are data and the solid histogram is signal MC simulation.

that background peaking under the signal comes from $J/\psi \to \gamma\eta'$, $\eta' \to \omega\gamma$, with the γ from the η' decay subsequently converting to an electron-positron pair. The distribution of the distance from the reconstructed vertex point of an electron-positron pair to the z axis, defined as R_{xy}, is shown in Fig. 3 (a). As expected from MC simulation of $J/\psi \to \gamma\eta'$, $\eta' \to \omega\gamma$, the peaks around $R_{xy} = 3$ cm and $R_{xy} = 6$ cm match the position of the beam pipe and the inner wall of the MDC, respectively, as shown in Fig. 3 (a). From the distribution of $M(e^+e^-)$ versus R_{xy} and the $M(e^+e^-)$ projections, shown in Figs. 3 (b) and (c), the requirement of $R_{xy} < 2$ cm can cleanly discriminate signal from the background. The number of peaking background events from $\eta' \to \omega\gamma$ that still survive is estimated to be 2.6±0.3 from MC simulation taking the branching fraction of $J/\psi \to \gamma\eta', \eta' \to \omega\gamma$ from this analysis, where the error is statistical. This background will be subtracted in the calculation of the branching fraction of $\eta' \to \omega e^+e^-$.

With all the above selection criteria being applied, the scatter plot of $M(\pi^0\pi^+\pi^-e^+e^-)$ versus $M(\pi^0\pi^+\pi^-)$ is shown in Fig. 4 (a), where the cluster in the η' and ω region corresponds to the decay $\eta' \to \omega e^+e^-$. The η' and ω peaks are clearly seen in the distributions of $M(\pi^0\pi^+\pi^-e^+e^-)$ (Fig. 4 (b)) and $M(\pi^0\pi^+\pi^-)$ (Fig. 4 (c)), respectively.

The same selection is applied to the inclusive MC sample of 1.2×10^9 J/ψ events to investigate possible background channels. The corresponding normalized distributions of $M(\pi^0\pi^+\pi^-e^+e^-)$ and $M(\pi^0\pi^+\pi^-)$ are shown as the histograms in Fig. 4 (b) and (c). One of the dominant backgrounds is from events with multiple π^0 in the final state with one π^0 undergoing Dalitz decay to γe^+e^-. Another important background, $\eta' \to \pi^+\pi^-\eta$, $\eta \to \pi^0\pi^+\pi^-$ with the pion pair from the η' decay misidentified as an electron-positron pair, produces an accumulation at the low mass region in the distributions of $M(\pi^0\pi^+\pi^-e^+e^-)$ and $M(\pi^0\pi^+\pi^-)$, and at the high mass region in $M(\pi^0\pi^+\pi^-e^+e^-)$-$M(\pi^0\pi^+\pi^-)$, which is shown as the shaded histograms in Fig. 4 (b), (c) and (d), normalized with the branching fraction from the PDG. The distribution of $M(\pi^0\pi^+\pi^-e^+e^-)$ - $M(\pi^0\pi^+\pi^-)$ is shown in Fig. 4 (d). From this study of the inclusive MC sample, no peaking background events are expected.

To determine the $\eta' \to \omega e^+e^-$ yield, an unbinned maximum likelihood fit to $M(\pi^0\pi^+\pi^-e^+e^-) - M(\pi^0\pi^+\pi^-)$, shown in Fig. 5, is performed. The signal component is modeled by the MC simulated signal shape convoluted with a Gaussian function to account for the difference in the mass resolution between data and MC simulation. The shape of the dominant non-resonant background $\eta' \to \pi^+\pi^-\eta$ is derived from the MC simulation, and its magnitude is fixed taking into account the decay branching fraction from the PDG [1]. The remaining background contributions are described with a 2nd-order Chebychev polynomial. The fit shown in Fig. 5 yields 66 ± 11 $\eta' \to \omega e^+e^-$ events with a statistical significance of 8σ. The statistical significance is determined by the change of the log-likelihood value and of the number of degrees of freedom in the fit with and without the $\eta' \to \omega e^+e^-$ signal included.

To determine the detection efficiency, we produce a signal MC sample in which $\eta' \to \omega e^+e^-$ is modeled as the decay amplitude in Ref. [2] based on the VMD model. After subtracting the peaking background events and taking into account the detection efficiency of (5.45±0.03)%, the branching fraction of $\eta' \to \omega e^+e^-$ is determined to be $(1.97 \pm 0.34) \times 10^{-4}$. This is summarized in Table I.

TABLE I. Signal yields, detection efficiencies and the branching fractions of $\eta' \to \omega\gamma$ and $\eta' \to \omega e^+e^-$. The first errors are statistical, and the second are systematical.

Decay mode	Yield	ε(%)	Branching fraction
$\eta' \to \omega\gamma$	33187 ± 351	21.87	$(2.55 \pm 0.03 \pm 0.16) \times 10^{-2}$
$\eta' \to \omega e^+e^-$	66 ± 11	5.45	$(1.97 \pm 0.34 \pm 0.17) \times 10^{-4}$

IV. SYSTEMATIC UNCERTAINTIES

In this analysis, the systematic uncertainties on the branching fraction measurements mainly come from the

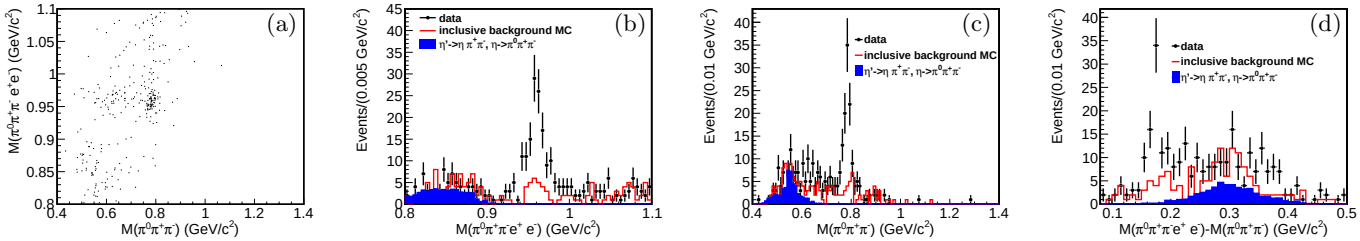

FIG. 4. (a) Distribution of $M(\pi^0\pi^+\pi^-e^+e^-)$ versus $M(\pi^0\pi^+\pi^-)$. (b) Invariant mass spectrum of $\pi^0\pi^+\pi^-e^+e^-$. (c) Invariant mass spectrum of $\pi^0\pi^+\pi^-$. (d) Distribution of $M(\pi^0\pi^+\pi^-e^+e^-) - M(\pi^0\pi^+\pi^-)$. The solid histogram represents the remaining events from the inclusive MC sample, and the shaded histogram shows misidentified events from the background channel $\eta' \to \eta\pi^+\pi^-$ normalized by using the branching fractions from the PDG [1].

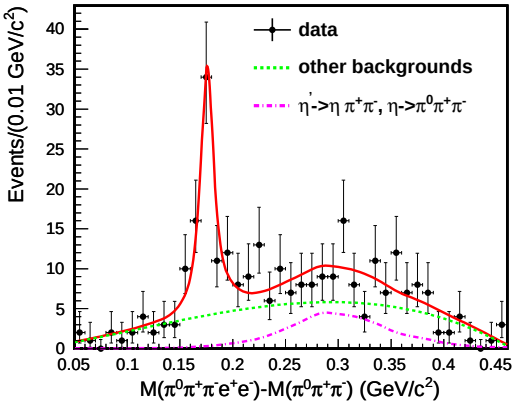

FIG. 5. Distribution of $M(\pi^0\pi^+\pi^-e^+e^-) - M(\pi^0\pi^+\pi^-)$ and the fit results. The crosses show the distribution of data. The dash-dotted line represents the $\eta' \to \pi^+\pi^-\eta$ component, and the dotted curve shows the background except $\eta' \to \pi^+\pi^-\eta$.

following sources:

a. MDC Tracking efficiency

The tracking efficiencies of pions and electrons have been investigated using clean samples of $J/\psi \to \rho\pi$, $\psi' \to \pi^+\pi^- J/\psi$, and $J/\psi \to e^+e^-(\gamma_{FSR})$. Following the method described in Ref [15], we determine the difference in tracking efficiency between data and simulation as 1% for each charged pion and 1.2% for each electron. Therefore, 2% is taken as the systematic error of the tracking efficiency for $\eta' \to \omega\gamma$ with two charged tracks, and 4.4% for $\eta' \to \omega e^+e^-$ with four charged tracks.

b. PID efficiency

For $\eta' \to \omega e^+e^-$, PID is used when we obtain χ^2_{4C+PID} of every combination for each event. The decay $J/\psi \to \pi^+\pi^-\pi^0$, with $\pi^0 \to \gamma e^+e^-$ is used as a control sample to estimate the difference between data and MC with and without applying χ^2_{PID} to identify the particle type. The difference, 3.8%, is taken as the systematic uncertainty from PID for the decay $\eta' \to \omega e^+e^-$.

c. Photon detection efficiency

The photon detection efficiency has been studied in $J/\psi \to \rho\pi$ decays in Ref. [15]. The difference between data and MC simulation is determined to be 1% per photon. Therefore, 4% and 3% are taken as the systematic uncertainties, respectively, for the two analyzed η' decays.

TABLE II. Summary of systematic uncertainties (in %) for the branching fraction measurements.

Sources	$\eta' \to \omega e^+e^-$	$\eta' \to \omega\gamma$	$\frac{\mathcal{B}(\eta'\to\omega e^+e^-)}{\mathcal{B}(\eta'\to\omega\gamma)}$
MDC tracking	4.4	2.0	2.4
Photon detection	3.0	4.0	1.0
PID	3.8	–	3.8
Kinematic fit	1.8	0.5	1.9
γ conversion subtraction	1.0	–	1.0
Background uncertainty	3.7	2.9	4.7
Form factor uncertainty	1.3	–	1.3
π^0 mass window	1.4	1.4	–
J/ψ total number	0.8	0.8	–
$\mathcal{B}(J/\psi \to \gamma\eta')$	3.1	3.1	–
$\mathcal{B}(\omega \to \pi^0\pi^+\pi^-)$	0.8	0.8	–
Total	8.7	6.4	7.0

d. Kinematic fit

The angular and momentum resolutions for charged tracks are significantly better in simulation than in data. This results in a narrower χ^2_{4c} distribution in MC than in data and introduces a systematic bias in the efficiency estimation associated with the $4C$ kinematic fit. The difference can be reduced by correcting the track helix parameters of the simulated tracks, as described in detail in Ref. [16]. In this analysis, a clean sample of $J/\psi \to \pi^+\pi^-\pi^0, \pi^0 \to \gamma e^+e^-$ is selected to study the difference of the helix parameters of pions and electrons between data and MC simulation. The helix parameters of each charged track are corrected so that χ^2_{4C} from MC simulation is in better agreement with that of data. With the same correction factors, the kinematic fit is performed for the signal MC events and the χ^2_{4C} is required to be less than 80. By comparing the numbers of selected signal events with and without the correction, we determine the change in detection efficiencies to be 0.5% and 1.8%. These are taken as the systematic uncertainties for $\eta' \to \omega\gamma$ and $\eta' \to \omega e^+e^-$, respectively.

e. γ conversion event veto

In the analysis of $\eta' \to \omega e^+e^-$, the large contamination of γ conversion events from the decay $\eta' \to \omega\gamma$ is effectively removed by the requirement of $R_{xy} < 2$ cm. To estimate the uncertainty associated with this requirement, we select a clean sample of $J/\psi \to \pi^+\pi^-\pi^0$ with $\pi^0 \to \gamma e^+e^-$. The efficiency corrected signal yields with and without the R_{xy} criterion differ by 1.0%, which is taken as the systematic uncertainty.

f. Background

The non-peaking background uncertainties in each channel are estimated by varying the fit range and changing the background shape in the fit, and they are determined to be 2.9% for $\eta' \to \omega\gamma$. To reduce the statistical uncertainty for $\eta' \to \omega e^+e^-$, we use the background shape from the inclusive MC sample, and the maximum change of the branching fraction, 3.6% is taken as the uncertainty from the non-peaking background. In order to evaluate the background uncertainty from $\eta' \to \eta\pi^+\pi^-$ in the analysis of the $\eta' \to \omega e^+e^-$ decay, to, we perform an alternative fit by varying its contribution according to the uncertainty from branching fractions of $J/\psi \to \gamma\eta'$ and its cascade decays. We also vary the selection efficiency of this background channel as determined by the MC sample, and find that the total difference in the signal yield is about 0.3%, which can be ignored. In addition, the change in the number of peaking background events from $\eta' \to \omega\gamma$ due to a difference of the γ conversion ratio between MC and data leads to an uncertainty of 1.0% on the branching fraction of $\eta' \to \omega e^+e^-$. The total background uncertainties from these sources are listed in Table. II.

g. Form factor

The nominal signal MC model is based on the amplitude in Ref. [2] To evaluate the uncertainty due to the choice of the form factors in the determination of the detection efficiency, we also generate MC samples with other form factors in Ref. [2], *e.g.*, the monopole and dipole parameterizations. The maximum change of the detection efficiency, 1.3%, is regarded as the systematic uncertainty from this source.

h. π^0 mass window requirement

The uncertainty from the π^0 mass window requirement due to the difference in the mass resolution between data and simulation is estimated by comparing the difference in efficiency of π^0 invariant mass window requirement between data and signal MC simulation. It is determined to be 1.4% for the $\eta' \to \omega\gamma$ mode. Since the π^0 kinematics in the $\eta' \to \omega e^+e^-$ decay is similar to the $\eta' \to \omega\gamma$ mode, the same value is taken as the uncertainty from this source for both decay modes.

The contributions of systematic uncertainties studied above and the uncertainties from the branching fractions ($J/\psi \to \gamma\eta'$ and $\omega \to \pi^+\pi^-\pi^0$) and the number of J/ψ events are summarized in Table II, where the total systematic uncertainty is obtained by adding the individual contributions in quadrature, assuming all sources to be independent.

V. RESULTS

The signal yields and detection efficiencies used to calculate the branching fractions and the corresponding results are listed in Table. I. Using the PDG world averages of $\mathcal{B}(J/\psi \to \gamma\eta')$ and $\mathcal{B}(\omega \to \pi^0\pi^+\pi^-)$ [1], the branching fractions of $\eta' \to \omega\gamma$ and $\eta' \to \omega e^+e^-$ are determined to be $\mathcal{B}(\eta' \to \omega\gamma) = (2.55 \pm 0.03(\text{stat})\pm0.16(\text{syst})) \times 10^{-2}$ and $\mathcal{B}(\eta' \to \omega e^+e^-) = (1.97 \pm 0.34(\text{stat})\pm0.17(\text{syst})) \times 10^{-4}$, respectively. The ratio $\frac{\mathcal{B}(\eta' \to \omega e^+e^-)}{\mathcal{B}(\eta' \to \omega\gamma)}$ is then determined to be $(7.71 \pm 1.34(\text{stat})\pm0.54(\text{syst})) \times 10^{-3}$, where several systematic uncertainties cancel, *e.g.*, the uncertainties associated with the charged pions (MDC tracking), photon detection efficiency, branching fractions of $J/\psi \to \gamma\eta'$ and $\omega \to \pi^+\pi^-\pi^0$ and the π^0 mass window requirement.

VI. SUMMARY

With a sample of 1.31 billion J/ψ events collected with the BESIII detector, we have analyzed the decays $\eta' \to \omega\gamma$ and $\eta' \to \omega e^+e^-$ via $J/\psi \to \gamma\eta'$. For the first time, the decay of $\eta' \to \omega e^+e^-$ is observed with a statistical significance of 8σ, and its branching fraction is measured to be $\mathcal{B}(\eta' \to \omega e^+e^-) = (1.97 \pm 0.34(\text{stat})\pm0.17(\text{syst})) \times 10^{-4}$, which is consistent with theoretical prediction, 2.0×10^{-4} [2]. The branching fraction of $\eta' \to \omega\gamma$ is determined to be $\mathcal{B}(\eta' \to \omega\gamma) = (2.55 \pm 0.03(\text{stat})\pm0.16(\text{syst})) \times 10^{-2}$, which is in good agreement with the world average value in Ref. [1] and the most precise measurement to date. In addition, the ratio $\frac{\mathcal{B}(\eta' \to \omega e^+e^-)}{\mathcal{B}(\eta' \to \omega\gamma)}$ is determined to be $(7.71 \pm 1.34(\text{stat})\pm0.54(\text{syst})) \times 10^{-3}$.

ACKNOWLEDGMENTS

The BESIII collaboration thanks the staff of BEPCII and the IHEP computing center for their strong support. This work is supported in part by National Key Basic Research Program of China under Contract No. 2015CB856700; National Natural Science Foundation of China (NSFC) under Contracts Nos. 11125525, 11235011, 11322544, 11335008, 11425524, 11175189; Youth Science Foundation of China under constract No. Y5118T005C; the Chinese Academy of Sciences (CAS) Large-Scale Scientific Facility Program; the CAS Center for Excellence in Particle Physics (CCEPP); the Collaborative Innovation Center for Particles and Interactions (CICPI); Joint Large-Scale Scientific Facility Funds of the NSFC and CAS under Contracts Nos. 11179007, U1232201, U1332201; CAS under Contracts Nos. KJCX2-YW-N29, KJCX2-YW-N45; 100 Talents Program of CAS; National 1000 Talents Program of China; INPAC and Shanghai Key Laboratory for Particle Physics and Cosmology; German Research Founda-

tion DFG under Contract No. Collaborative Research Center CRC-1044; Istituto Nazionale di Fisica Nucleare, Italy; Ministry of Development of Turkey under Contract No. DPT2006K-120470; Russian Foundation for Basic Research under Contract No. 14-07-91152; The Swedish Resarch Council; U. S. Department of Energy under Contracts Nos. DE-FG02-04ER41291, DE-FG02-05ER41374, DE-FG02-94ER40823, DESC0010118; U.S. National Science Foundation; University of Groningen (RuG) and the Helmholtzzentrum fuer Schwerionenforschung GmbH (GSI), Darmstadt; WCU Program of National Research Foundation of Korea under Contract No. R32-2008-000-10155-0.

[1] K. A. Olive *et al.* (Particle Data Group), Chin. Phys. C **38**, 1 (2014).
[2] A. Faessler, C. Fuchs, M. Krivoruchenko, Phys. Rev. C **61**, 035206 (2000).
[3] M. Ablikim *et al.*, (BESIII Collaboration), Phys. Rev. D **87**, 092011 (2013).
[4] B. Borasoy, R. Nissler, Eur. Phys. J. A **33**, 95 (2007).
[5] C. Terschlüsen, S. Leupold, M. Lutz, Eur. Phys. J. A **48**, 190 (2012).
[6] M. Ablikim *et al.* (BESIII Collaboration), Chin. Phys. C **36**, 915 (2012).
[7] With the same approach as for J/ψ events taken in 2009 (see Ref. [6] for more details), the preliminary number of J/ψ events taken in 2009 and 2012 is determined to be 1310.6×10^6 with an uncertainty of 0.8%.
[8] M. Ablikim *et al.* (BESIII Collaboration), Nucl. Instrum. Meth. A **614**, 345 (2010).
[9] S. Agostinelli *et al.*, Nucl. Instrum. Meth. A **506**, 250 (2003).
[10] J. Allison, K. Amako, J. Apostolakis, H. Araujo, P. Dubois *et al.*, IEEE Trans. Nucl. Sci. **53**, 270 (2006).
[11] S. Jadach, B. Ward, Z. Was, Comput. Phys. Commun. **130**, 260 (2000).
[12] S. Jadach, B. Ward, Z. Was, Phys. Rev. D **63**, 113009 (2001).
[13] D. J. Lange, Nucl. Instrum. Meth. A **462**, 152 (2001); R. G. Ping, Chin. Phys. C **32**, 599 (2008).
[14] J. C. Chen, G. S. Huang, X. R. Qi, D. H. Zhang, Y. S. Zhu, Phys. Rev. D **62**, 034003 (2000).
[15] M. Ablikim *et al.* (BESIII Collaboration), Phys. Rev. D **83**, 112005 (2011).
[16] M. Ablikim *et al.* (BESIII Collaboration), Phys. Rev. D **87**, 012002 (2013).